Polymer Bulletin
https://doi.org/10.1007/s00289-022-04400-1

ORIGINAL PAPER

Synthesis of calcium carbonate-quince bio-composite for programmed and on-demand drug release of paracetamol at target site: a green chemistry approach

Rija Kulsoom[1] · Muhammad Sarfraz[1] · Attia Afzal[1] · Muhammad Farooq[1] · Sherjeel Adnan[1] · Muhammad Umer Ashraf[1] · Shujat Ali Khan[2]

Received: 12 September 2021 / Revised: 5 April 2022 / Accepted: 18 July 2022

Abstract

In this study, an inorganic–organic composite system was developed through biomineralization of calcium carbonate in the quince-seed mucilage-based hydrogel. Drug-polymer interactions were studied by FTIR, DSC, XRD and SEM analysis. The water absorption capacity was calculated by swelling index. Drug release was determined at various pH. Several in vitro kinetic models were applied to observe drug release behaviour. Studies of drug-polymer interactions and particle flow characteristics of the developed composite material have shown that there is good compatibility between drug and the excipients. The XRD and SEM results confirmed calcite polymorphs in the developed composite material. Thermograms showed that the developed composite material was heat stable. A restricted drug release was observed in an acidic medium (pH 1.2). A controlled drug release was depicted from the developed system at pH 6.8. The drug release mechanism of Super Case II was suggested. The developed system was considered to be an effective drug carrier for colon targeted oral delivery of non-steroidal anti-inflammatory drugs (NSAIDs) to avoid gastric irritation and risk of ulceration.

Rija Kulsoom, Muhammad Sarfraz and Attia Afzal have contributed equally in this manuscript.

✉ Muhammad Sarfraz
chiefpharm@gmail.com

✉ Attia Afzal
attiapharm@gmail.com

[1] Lahore School of Pharmaceutical Sciences (LSPS), Faculty of Pharmacy, The University of Lahore, Lahore 54600, Punjab, Pakistan

[2] Department of Pharmacy, COMSATS University Islamabad, Abbottabad Campus, Abbottabad 22060, KPK, Pakistan

Published online: 30 July 2022

Graphical abstract

An illustration of extraction of quince hydrogel and development of calcium carbonate-quince ($CaCO_3$-Q) composite system; QSM = Quince seed mucilage

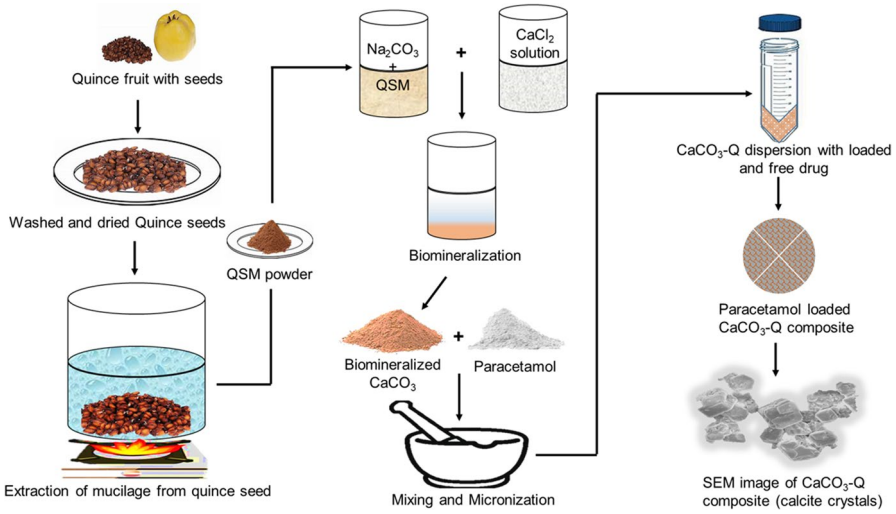

Keywords $CaCO_3$-qunice composite, inorganic–organic composite · Polymer composites · Biomineralization · Paracetamol

Introduction

Acetaminophen, commonly called Paracetamol, is one of the most used medicines in children for fever management and mild-to-moderate pain. It is considered first line of defence against fever and mild pain and is included in the List of Essential Medicines for Children by the World Health Organization (WHO) [1]. Market research report shows several folds increase in use of paracetamol due to increasing trend of flu and flu like symptoms and pain management [2]. Moreover, the current ongoing COVID-19 pandemic is also a contributing factor for over use of paracetamol among the patients to reduce fever [3, 4]. Even though paracetamol is considered safer drug for infants and children, it can cause severe liver toxicity if taken in large amounts [5]. Due to the parents' anxiety and fever phobia associated with current COVID-19 pandemic, there is a high risk of unintentional overdosing of paracetamol in children. Paediatric drug metabolism differs from adult metabolism. Children have a larger liver size compared to their body weight than adults, resulting in a higher drug metabolism rate [6]. In case of an overdose, the majority of paracetamol is metabolized to N-acetyl-p-benzoquinone imine, which is responsible for liver toxicity. Paracetamol toxicity is the second most common cause of liver transplantation in the world and the most common in the USA [7].

The elimination half-life ($t½$) of paracetamol is approximately of 2 h with therapeutic doses [8]. Moreover, paracetamol is very slightly soluble in cold water but greater solubility in hot water. This solubility may further decrease in the presence of various excipients. For example, during development of sustained release tablet formulations, a 20–30% decrease in solubility was observed when paracetamol was blended with water-soluble excipients such as potassium bicarbonate, sodium bicarbonate, and sodium chloride [9]. The body mass formula, the use of milligram per Kg, is commonly used for the adjustment of dose for children. In this context, for accurate dosing, the flexible formulations such as drops and syrups are preferred over solid dosage forms for children. To get therapeutic benefits, paracetamol-based oral formulations are given in 3-4 divided doses over the day. However, non-cooperative, unwilling and frightened behaviour of the children for medication may lead to wrong and over doses of these flexible formulations. Controlled release liquid preparation approaches are getting attention of the researchers to provide a rational product for lower age patients (children and infants) to improve further patient compliance by reducing dose frequency.

Clinical pharmacokinetic studies of the paracetamol reveal that the rate of oral absorption of this drug is predominantly dependent on the rate of gastric emptying; being delayed by the presence of food in the stomach [10, 11]. Although paracetamol is a weak acidic drug that remains unchanged in stomach, it absorbs more rapidly from small intestine [11]. The children are more likely to eat food several times in a day including eating of junk foods in a daily life. Hence, the administration of conventional oral formulations of paracetamol in divided doses may be one of the reasons of increasing incidence of liver toxicity in early (children) and late age (old). Considering above stated drug-related issues such as shorter half-life (2 h) and its oral conventional formulations-related concerns (dose adjustment due to non-cooperative attitude of the children), here, we propose sustained release dried oral suspension of paracetamol to achieve patient compliance and enhanced oral absorption from small intestine. Oral dried formulations can be easily packed in a single divided dose sachets to improve product stability and patient compliance.

Green chemistry is an area of research to develop environment friendly products without using hazardous chemicals or substances. This approach is also getting attention of the pharmaceutical industries to develop a carrier system that should be biocompatible with our system in order to deliver the drugs at a target site. Gelling materials on contact with aqueous medium form three-dimensional structure (gel formation) that depends on type of bond formation within the network. In this context, gel are classified into two major categories: physical and chemical gel. The physicochemical characteristics of this three-dimensional network can be modified by crystallization of inorganic materials in the gel. Crystal growth in hydrogels is tremendously getting attention of researchers to design modified matrix systems for biomedical applications. Bio-mineralized crystal formation depends on its microenvironment such as composition and concentration of biomacromolecules (gelling agent), pH, incubation period, inorganic and organic ratio [12]. Aside by microenvironment, the methodology of biomineralization process, for example, mixing of previously formed crystals with sol, so-called internal gelation, or precipitation of crystals after gelation, also influences the behaviour of gel network. The crystallization

of calcium carbonate in hydrogels of natural polymers such as agarose, xanthan, gelatin and chitosan was investigated for structural, morphological and physicochemical changes in gel network [13]. Some studies have also demonstrated the influences of additives/surfactant such as inulin, alkonamide, poloxamer, lipopeptide, aspartic acid and lysine on the shape, size, adsorption rate, porosity and precipitation kinetics of biomineralized calcium carbonate crystals [14–19]. The drug loading and drug targeting via calcium carbonate crystallization in natural polyscharides such as pectinalginate, hyaluronate, and synthetic biomolecules such as dextran sodium sulphate (DSS) and polyarginine (PARG), have been reported [20–24]. No studies have reported calcium carbonate crystallization in hydrogels obtained from gums or mucilage.

Gums and mucilages from plant origin (green chemistry) behave like hydrogel and their gelling behaviour is believed to dependent on nano-scale 3D-networks [25, 26]. In most cases, these gums and mucilages are composed of macromolecules typically polysaccharides and proteins with glycosidic and amino acid repeating unit. Natural materials have advantage over synthetic materials due to their biosafety, abundance and economy [27]. A tree plant (Cydonia Oblonga) from *Rosaceae* family commonly known as quince is native to Middle East, Iran, South Asian regions and Europe. The aqueous extract of quince seeds contains glucuronoxylan. The glucuronoxylan hydrogel extracted from quince seeds contains a high percentage of glucuronic acid residue and xylose [28, 29]. It dissolves and swells up readily in water. It is considered a potential candidate for controlled drug release [30]. The quince mucilage, a source of high quality nanofibrillar cellulosic materials, has good mechanical properties that make it attractive to build novel bio-materials and composite structures [31]. A pH responsive swelling behaviour of quince mucilage was observed; significant swelling was observed in a basic media, while insignificant swelling was observed in an acidic media [32]. Quince-seed mucilage was used as a stabilizer in emulsion preparation and green synthesis of zinc oxide nanoparticles and as a bioabsorbant to remove calcium ions from solution [33–35]. Whey protein-quince seed mucilage coaservates have been designed and investigated for change in physicochemical properties of the resultant hydrogel [36]. Hence, quince mucilage is proposed an ideal material for drug targeting and building block for new materials or composite structures.

Porous inorganic mono-structured materials have been used as drug carriers because of their unique features such as large surface area, porosity, and stability in biological fluids [37]. Among inorganic materials, calcium carbonate is widely used in biomedical research because of its low cost, bio-safety, biocompatibility and pH sensitivity. However, calcium carbonate is practically insoluble in water, which limits its scope to develop oral liquid preparations. Here, we propose crystallization of calcium carbonate in the quince mucilage-based hydrogels to develop a novel composite system for programmed and on-demand release of paracetamol at target site (intestine). We expect that biomineralized calcium carbonate will improve drug loading, biocompatibility and controlled drug release in the small intestine. At the same time, quince hydrogel exists in the internal and external environment of biomineralized calcium carbonate crystals that will restrict the drug leakage in stomach due to switch off properties of quince hydrogel in the acidic environment.

The proposed calcium carbonate-quince composite will be an attractive biomaterial for sustained release oral delivery of paracetamol in the small intestine and will improve 'patient compliance' in the lower age patients (children and infants) by reducing dose intervals.

Experimental

Materials

Quince gel was extracted from quince seeds purchased from local market of Lahore, Pakistan. Sodium carbonate and potassium dihydrogen phosphate were imported from Riedel–de Haen and Merck in Germany. Calcium chloride, sodium hydroxide and HCl were imported from BDH Laboratory supplies located in England. Paracetamol was gifted from WIMITS pharmaceuticals situated in Lahore, Pakistan. Methanol was imported from Emirgul Gida, Turkey. The deionized water used was prepared in laboratories of The University of Lahore.

Extraction of quince hydrogel

Clean quince seeds of 100 g weight were taken. These unsoiled seeds were soaked in 500 mL of deionized water for 2–3 days and heated at 50 °C for 30 min on a hot water bath leading to complete extrusion of quince hydrogel. Later, the obtained viscous gel was strained through cotton cloth to remove seed and seed debris. The strained gel was washed thrice with n-hexane to remove lipophilic contents. Gel was dried in an oven at 60 °C for 2 to 3 days. Flaky dried gel was obtained, grinded in a pestle and mortar to get fine powder and stored in an airtight container.

Crystallization of calcium carbonate in quince hydrogel

Dried quince hydrogel powder was dissolved in 50 mL of Na_2CO_3 (0.2 M) while heating at 70–80 °C with continuous stirring on a hot water bath. In the meanwhile, 50 mL of $CaCl_2$ (0.2 M) was prepared and rapidly mixed in the above solution. A milky appearance (turbidity) was observed at the time of mixing both solutions that was an indication of crystallization of calcium carbonate. The suspension was then left at room temperature for 5 days. Later, the obtained colloidal dispersion was centrifuged at 5000 × g for 10 min followed by washing of precipitate with saturated calcite solution several times and dried at 60 °C for 3 h at the end of each experiment. The obtained dried dispersion was called calcium carbonate-quince ($CaCO_3$-Q) crystals. Following above stated procedure, three formulations were prepared containing 0.005%, 0.05% and 0.5% of dried quince hydrogel powder in final colloidal dispersion, designated as F′1, F′2, and F′3, respectively.

Drug loading

$CaCO_3$-Q crystals and paracetamol powder were grinded together in a mortar and pestle at a ratio of 70:30 (w/w), respectively. This mixture was dissolved in 5 mL distilled water and stirred on a hot plate magnetic stirrer for 48 h. To remove unentrapped drug, the resultant dispersion was centrifuged at 5000 × g for 10 min. Supernatant was collected and subjected to UV analysis to quantify free paracetamol, while paracetamol-loaded $CaCO_3$-Q crystals were collected and dried in an oven at 60 °C for 2 h. The drug-loaded formulations were designated as F1, F2 and F3 in correspondence to $CaCO_3$-Q crystal formulations (F′1, F′2 and F′3).

Micromeritics of dried calcium carbonate-quince crystals

Physical and mechanical properties of the developed $CaCO_3$-Q crystals were studied. Bulk density, tapped density, compressibility index, Hausner's ratio, and angle of repose are computed by the following formula:

$$\text{BulkDensity} = \frac{M}{V_\text{b}} \tag{1}$$

$$\text{Tapped density } = d_\text{t} = \frac{M}{V_\text{t}} \tag{2}$$

$$\text{Compressibilityindex} = \frac{d_{\text{t}-d_\text{b}}}{d_\text{t}} \times 100 \tag{3}$$

$$\text{Hausner's ratio} = \frac{d_\text{t}}{d_\text{b}} \tag{4}$$

$$\text{Angle of repose } = \theta = \tan^{-1}\frac{h}{r} \tag{5}$$

where M: mass of powder, V_b: bulk volume of powder, V_t: tapped volume of powder, $D_{\text{t: tapped}}$ density of powder, D_b: bulk density of powder, r: radius of powder, h: height of powder.

For results and discussion of micromeratic studies, see "supplemental material."

Drug content determination

With some modification, drug content was measured as reported [38]. Briefly, drug-loaded $CaCO_3$-Q crystals were dispersed in phosphate buffer pH 6.8 with 0.1% sodium lauryl sulphate (SLS) and stirred for 24 h. The resultant suspension was centrifuged at 5000 × g for 5 min, and the supernatants were filtered through 0.45 µm.

The filtrate was diluted as desired and drug content was quantified by UV spectrophotometer at 243 nm [39]. Following equation is used to calculate entrapment efficiency (E.E.) of the drug.

$$\text{E.E.} = \frac{\text{initial amout of drug loaded} - \text{free amount of drug in supernentant}}{\text{ininitial amount of drug loaded}} \times 100 \tag{6}$$

Swelling index

Cellophane bags were charged by soaking them in distilled water for 2–3 min. After that, water was drained off and empty bags were dried in an oven. A 200 mg of drug-loaded $CaCO_3$-Q crystals were packed in the dried cellophane bag and immersed in water (50 mL). After 1 h, the bags were removed from water, the excess water was drained off and the bags were weighed. Swelling index is calculated by the formula [28]:

$$\text{swellingindex } (g/g) = \frac{w_s - w_e - w_i}{w_i} \tag{7}$$

w_s = weight of filled cellophane bag (swollen $CaCO_3$-Q), w_e = weight of empty cellophane bag, w_i = initial weight of gel.

Drug polymer interaction studies

Fourier transform-infrared spectroscopy (FTIR)

Relevant bonds and functional groups of representative materials were determined by FTIR spectra. The spectrum was composed of between 400 and 4000 cm^{-1} with an average spectral resolution of 32 scans of 2 cm^{-1}.

Differential scanning calorimetry (DSC)

DSC analysis was performed to examine thermal behaviour of drug and the developed colloidal systems. A PerkinElmer DSC-7 thermal analyzer was used to perform differential scanning calorimetry. Samples were heated between 50 and 250 °C at a rate of 10 °C/min.

X-ray diffraction analysis (XRD)

X-ray diffractometer (Bruker DH, Germany) was used to observe crystal symmetry and phase. XRD patterns determine parameters of crystal lattice. Scherer's formula was used to calculate the size of the crystals [40]. The recording time was 6 min for scanning.

Scanning electron microscopy (SEM)

Surface morphology of drug-loaded $CaCO_3$-Q crystals was examined using 0.5–1 kV scanning electron microscope (SEM; HITACHI SU8030, Japan). Before observation, the samples were placed on a stub made of aluminium in an argon atmosphere under vacuum. Particle size, shape and texture of samples were evaluated at different magnifications.

In vitro dissolution

A 5 mg of drug-loaded $CaCO_3$-Qcrystals were dispersed in 1 mL of dissolution media inside a dialysis bag (molecular weight cut-off 14,000 Da) which was tied at both ends and immersed in 100 mL of dissolution media with continuous stirring at 37 °C. A sample of 3 mL was withdrawn at each time point after specific intervals, while the volume of the dissolution media was maintained with fresh media. Dissolution study was conducted in 0.1 N HCl (pH 1.2) and phosphate buffer solution (pH 6.8) and drug content was quantified by UV at 243 nm.

Following in vitro kinetic models were applied to see drug release behaviour from the developed composite systems:

$$\text{Zero order} \quad Q = Q_\circ + K_\circ t \tag{8}$$

$$\text{First order} \quad \log \mathrm{Q} = \log \mathrm{Q}_\circ - \mathrm{Kt}\,2.303 \tag{9}$$

$$\text{Higuchi} \quad f = Q = A\sqrt{D\left(2\mathrm{Q}_\circ - \mathrm{Q}s\right)\mathrm{Q}st} \tag{10}$$

$$\text{Hixon-Crowell} \quad Q_\circ^{1/3}/Q_t^{1/3} = K_{\mathrm{HC}}t \tag{11}$$

$$\text{Korsmeyer} - \text{Peppas} \quad Q_t/Q_\circ = K_t^n \tag{12}$$

$$\text{Weibull} \quad \mathrm{Qt}/Q_\circ = 1 - e^{-K(t-T)} \tag{13}$$

$$\text{Gompertz} \quad Q_t/Q_{\max} = \mathrm{Exp}\left[-e^{\beta \log t}\right] \tag{14}$$

$$\text{Logistic} \quad Q = A/1 + e^{-k(t-y)} \tag{15}$$

$$\text{Probit} \quad Q = \Phi(+\beta.\log(t)) \tag{16}$$

where $Q_\circ$: initial amount of drug added, Q_t: drug release in time t, T: lag time, $K_\circ$: rate constants for zero order, K: first-order rate constant, D: diffusion of the drug molecules, Q s: solubility of drug in the matrix medium, $\mathrm{K_{HC}}$: rate constant for

Hixson-Crowell rate equation, n: release exponent and Φ: standard normal cumulative distribution function.

Note: Korsmeyer-Peppas and Weibull models were fitted to first 60% drug release data. In case of Korsmeyer-Peppas model, the value of n represents the release mechanism of drug as stated in Table 1.

Statistical analysis

In vitro kinetic model parameters were computed by DDSolver add-in program for excel. Group comparison was done by one-way analysis of variance (ANOVA) with Bonferroni's Multiple Comparison Test ($P < 0.05$).

Results and discussion

Preparation of $CaCO_3$-Q composite, drug loading and entrapment efficiency

Calcium carbonate-quince ($CaCO_3$-Q) composite systems were developed by biomineralization of calcium carbonate in various concentrations of quince hydrogel. The developed CaCO3-Q composites were characterized for drug loading and entrapment efficiency.

No interfering peak was observed in UV scan (data not shown). Entrapment efficiency of drug in the developed formulations F1, F2 and F3 was $94 \pm 0.04\%$, $85 \pm 0.05\%$, and, $80 \pm 0.06\%$, respectively. These results revealed that as the concentration of quince hydrogel was increased, the drug entrapment efficiency was decreased. Quince seed mucilage (QSM) contains large proportion of water-soluble hemicelluloses, thus increase in QSM concentration may brought changes in viscoelastic behaviour of the resultant matrix for possible variation in drug loading.

Swelling index

The degree of swelling of pure quince gel powder and drug-loaded $CaCO_3$-Q crystals were determined in deionized water. The pure quince seed mucilage hydrogel at concentration of 0.5% (w/v) showed swelling index of 190%. Swelling index of formulations F′1, F′2 and F′3 was 125%, 150% and 350%, respectively, as shown in Fig. 1. Our results were correlated with the previous study in which more swelling was observed at higher concentration of quince gel due to higher proportion of

Table 1 Diffusional release mechanisms from swellable systems

Release exponent (n)	Drug release mechanism
$n = 0.45$	Fickian diffusion
$0.45 < n < 0.89$	Non-Fickian diffusion
$= 0.89$	Case II transport
$n > 0.89$	Super Case II transport

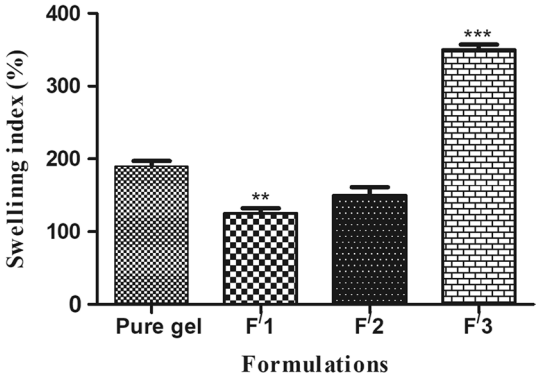

Fig. 1 Swellable capacity of the developed calcium carbonate-quince ($CaCO_3$-Q) composites; F′1 = unloaded $CaCO_3$-Q composite containing 0.005% quince c F′2 = unloaded $CaCO_3$-Q composite containing 0.05% quince d F′3 = unloaded $CaCO_3$-Q composite containing 0.5% quince

deprotonation of carboxyl group of polysaccharides at basic or neutral pH. Similarly, the higher swelling behaviour is also associated with the presence of greater number of carboxylate ions in the solution that produces more repulsion [32]. Such high values of swelling index make quince hydrogel an excellent candidate to be used as binder, disintegrating and matrix agent for sustained release dosage forms [41]. Moreover, swelling and deswelling behaviour at different pH made it a suitable candidate for stimuli response drug delivery systems [42]. A significant difference in swelling index was observed between pure quince hydrogel and its corresponding biomineralized calcium carbonate composites. The swelling index was increased twofold at 0.5% concentration of quince hydrogel powder (F′3 formulation). The increase in the swelling index was obviously due to increase in porosity by calcium carbonate. Therefore, more swelling was observed in the developed hollow composite fabric network as compared to pure hydrogel [43]. Although the swelling index was less than of pure hydrogel in formulation F′1 but it was equal to pure hydrogel in formulation F′2. In fact, an optimum inorganic to organic ratio is desirable for complete biomineralization process. Time is also an important factor in crystal growth. The lower swelling index of F′1 formulation might be due to incomplete biomineralization.

Drug-polymer interaction studies

Fourier transform infrared (FTIR) spectroscopy

Figure 2 represents the FTIR spectrum of the developed composite (CaCO3-Q).

Quince hydrogel which is composed of large number of hemicelluloses showed distinct peaks at 1041 cm^{-1} which refer to glyosidic linkage at polysaccharide unit, as visible in FTIR pattern given in Fig. 2A(a) and B(a). Carbonyl group (C = O) is attributed to the peak appeared at wave number 1410 and 1610 cm^{-1}. All these characteristic peaks of glycosidic linkage and C = 0 suggested the polysaccharide arrangement of quince hydrogel [32].

The most prominent peak of pure drug, i.e. paracetamol was visible at wave number 1600 cm^{-1} and 1650 cm^{-1} which were attributed to C = C and C = O stretching,

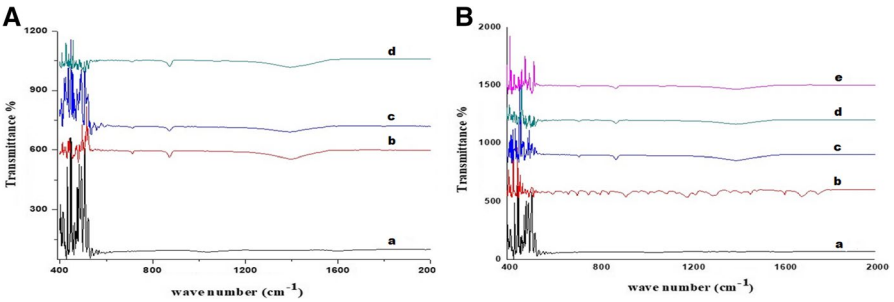

Fig. 2 FTIR spectra of quince mucilage, paracetamol and $CaCO_3$-Q composites **A** unloaded $CaCO_3$-Q composite a) quince seed mucilage; b) F′1 = unloaded $CaCO_3$-Q composite containing 0.005% quince c) F′2 = unloaded $CaCO_3$-Q composite containing 0.05% quince d) F′3 = unloaded $CaCO_3$-Q composite containing 0.5% quince **B** drug-loaded $CaCO_3$-Q composite a) quince seed mucilage; b) paracetamol c) F1 = drug-loaded $CaCO_3$-Q composite containing 0.005% quince d) F2 = drug-loaded $CaCO_3$-Q composite containing 0.05% quince e) F3 = drug-loaded $CaCO_3$-Q composite containing 0.5% quince

respectively. The peak at 1580 cm^{-1} is due to N–H bending. Asymmetrical C–H bond bending and C–C stretching were assigned to 1490 cm^{-1} and 1440 cm^{-1}. The peaks having wave numbers 1324 cm^{-1} and 1285 cm^{-1} were attributed to symmetrical C-H bending and C–N stretching. The wave number 1041 cm^{-1} corresponds to CH_3 rocking. Absorption peaks at 935 cm^{-1} and 1100 cm^{-1} were assigned to C–N and C = O stretching. Vibrational peaks at 580 cm^{-1} and 860 cm^{-1} were characterized for phenyl and aromatic ring, respectively. Aforesaid description of the peaks and the bands associated with FTIR of paracetamol was consistent with the literature [44–46], asshown in Fig. 2B(b).

Although, the above stated distinct peaks of quince hydrogel and pure drug (paracetamol) were disappeared after biomineralization process that was correlated with the observation of the other researcher [47]. However, the distinct peaks of calcium carbonate at wave numbers 710 cm^{-1} and 855 cm^{-1} were observed; attributing symmetric in and out plane bending mode of carbonate ion, respectively. The spectral data revealed broad absorption peak at 1410 cm^{-1} which confirmed asymmetric stretching mode of carbonate (C–O) [48], as shown in Fig. 2A(b, c, d) and Fig. 2B(c, d, e). These carbonate ion-associated peaks demonstrated growth of biomineralized calcium carbonate crystals that were calcite in nature as confirmed by XRD analysis and SEM images, discussed later.

Differential scanning calorimetry (DSC)

Differnetial scanning calorimetry is effectively used to check the thermal stability of polymers and polymer-based products. The melting point can be determined by the melting curve. The first endothermic peak appeared at 140 °C in DSC heating curve; indicating loss of adsorbed and structural water of the pure gel (qunice mucillage), as shown in Fig. 3A. The second and third enothermic peaks at around 200 °C suggested complete decomposition of the gel networks. No enothermic peask was observed in the DSC heating curve of unloaded

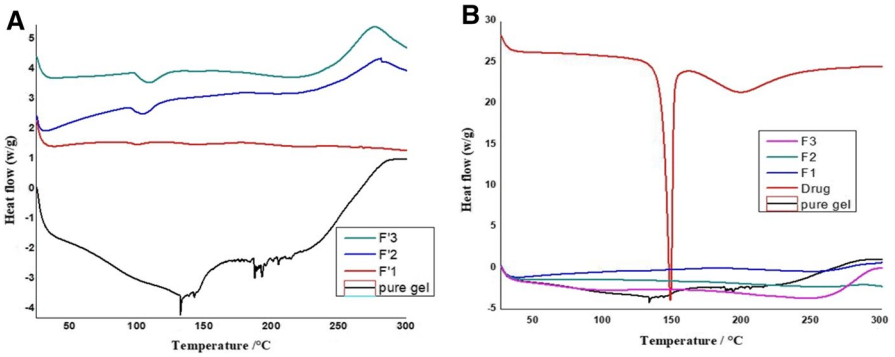

Fig. 3 Thermogram of the developed calcium carbonate-quince ($CaCO_3$-Q) composites **A** unloaded $CaCO_3$-Q composite F′1 = unloaded $CaCO_3$-Q composite containing 0.005% quince; F′2 = unloaded $CaCO_3$-Q composite containing 0.05% quince; F′3 = unloaded $CaCO_3$-Q composite containing 0.5% quince **B** drug-loaded $CaCO_3$-Q composite F1 = drug-loaded $CaCO_3$-Q composite containing 0.005% quince; F2 = drug-loaded $CaCO_3$-Q composite containing 0.05% quince; F3 = drug-loaded $CaCO_3$-Q composite containing 0.5% quince

compoite sytem (F′1, F′2 and F′3), except at 100 °C; suggesting water loss due to evaporation only. A wide exothermic peak was also observed in F′2 and F′3 formulaitons; indicating structural changes in gel network due to poosible ionic and hydrogen bond formation in the presence of mono (Na^+) and divaelnt (Ca^{++}) ions during biomineralization process. It is well understood that bond energy for ionic bond is higher than the hydrogen bonding [49]. It was obviously due to the deposition of biomineralized calcium carbonate crystals in the hydrogel which brought more stable networks. However, the resultant composite system at 0.005% of quince hydrogel (F′1 formulaiton) practically behaved like pure calcium carbonate. No exothermic peak was observed in the DSC thermogram of F′1 formulaiton as shown in Fig. 3A. Crystalline calcium carbonate is stable at this study temperature range (0–300 °C); while calcium carbonate shows thermal decompsoiton (endothermic peak) only at high temperature (800 °C) [50].

Paracetamol exhibits a number of transitions between different forms and the behavior is not always reproducible. The DSC is needed to understand the relationship between the different forms. The pure paracetamol thermogram showed endothermic peak at temperature 147 °C which represents the melting temperature of paracetamol, as shown in Fig. 3B. It was demostrated that the pure paracetamol sample is converted to Form I nearly at about 120 °C and then melted at 170 °C. The amorphous glass underwent the expected transitionafter cooling to Form III and then to Form II. The conversion from Form II to Form I is not always visible [51].

In contrast to unloaded composite systems, the drug-loaded compsoite systems (F1, F2, and F3) did not show enndothermic peaks. Hence, the developed system was suggested heat stable which can protect drug from thermal degradation.

X-ray diffraction (XRD)

X-ray diffraction study was carried out to investigate crystallographic nature of the calcium carbonate polymorphs produced during the biomineralization in quince gel, before and after drug loading. Calcium carbonate exists in three polymorphs in nature: vaterite, aragonite and calcite. Vaterite is relatively less stable than aragonite and calcite. Vaterrite is transformed to arganoite in 1 h at 60 °C and to calcite in 24 h at room temperature [52]. Each polymorph has unique surface morphology which can be identified by the SEM study. However, SEM analysis is not conclusive to discriminate calcium carbonate polymorph because shape of calcium carbonate crystals changes in different crystallization condition. For example, aragonite is needle-like but it may be flake-like or cauliflower-like at different micro-environment conditions [53]. Quince seed mucilage was pertained to crystalline nature by two broad peaks at $2\theta = 20.2°$ and 24.1° [33, 54]. Low intensity sharp peaks of intensity > 1000a.u between 20° and 23° were observed that could confirm mild crystalline nature of pure quince gel sample. Among all peaks, three distinct peaks of intensity 1370, 1356 and 1332 were observed at diffraction angle of 21.98°, 22.38°, and 22.14°, respectively. Results revealed high crystalline change in gel network after biomineralization of calcium carbonate that was evidenced by the presence of sharp peaks in the XRD pattern. The drug unloaded formulations F′1, F′2, F′3 showed high intensity peaks of 13,229 a.u., 7565 a.u. and 6174 a.u. at 29.42°, 29.38° and 29.46°, respectively (Fig. 4A). The drug-loaded formulations F1, F2, and F3 have their sharpest peaks at angles 29.38°, 29.46° and 29.42° with an intensity of 8403 a.u., 4173 a.u. and 7438 a.u., respectively. XRD patterns were compared with XRD patterns of calcium carbonate polymorph standards [55] that confirmed the biomineralized calcium carbonates which were calcite in their crystallographic

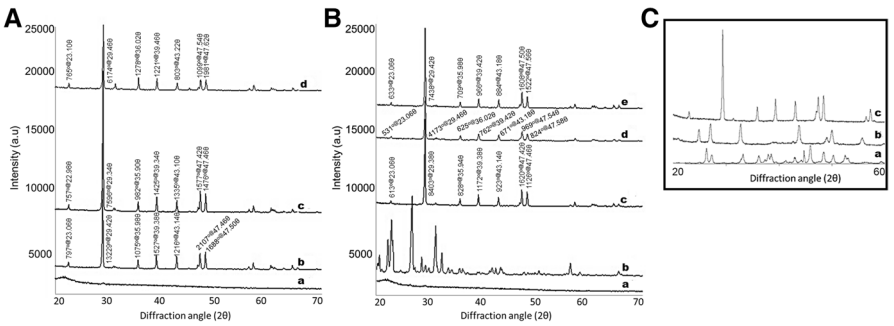

Fig. 4 Diffractogram of the developed calcium carbonate-quince ($CaCO_3$-Q) composites **A** unloaded $CaCO_3$-Q composite a) quince seed mucilage; b) F′1 = unloaded $CaCO_3$-Q composite containing 0.005% quince c) F′2 = unloaded $CaCO_3$-Q composite containing 0.05% quince d) F.′3 = unloaded $CaCO_3$-Q composite containing 0.5% quince (**B**) drug-loaded $CaCO_3$-Q composite a) quince seed mucilage; b) paracetamol c) F1 = drug-loaded $CaCO_3$-Q composite containing 0.005% quince d) F2 = drug-loaded $CaCO_3$-Q composite containing 0.05% quince e) F3 = drug-loaded $CaCO_3$-Q composite containing 0.5% quince **C** XRD pattern of calcium carbonate polymorphs a) aragonite b) vaterite c) calcite [published by Ming Ni and Buddy D. Ratner, a courtesy of Surf Interface Anal. 2008 Oct; 40(10): 1356–1361. 10.1002/sia.2904]

behaviour as the most intense peak of calcite polymorph appeared around 30° (file JCPDS no. 5-586) [56], as shown in Fig. 4B.

No significant difference of angular location was observed before and after loading of drug. Hence, there was no chemical interaction between drug and biopolymers of the gel. Although reduction in peak intensities after drug loading was observed that meant crystallinity of the formulations reduced that was might be due to incorporation of drug (amorphous/mild crystalline in nature). On the basis of observed highest peak intensity, unloaded and drug-loaded formulations follow order $F'1 > F'2 > F'3$ and $F1 > F3 > F2$, respectively. It suggested that $F'1$ (a member of unloaded formulation group) and F1 (a member of drug-loaded formulation group) formulations were more crystalline than the rest of the group members. It was inferred from the results that as the concentration of gel powder was increased; crystallinity of the corresponding formulations was decreased because of amorphous nature of gel powder.

Pure paracetamol (drug) presented sharper peaks of intensity 3590 a.u, 5396 a.u, 7563 a.u, 1243 a.u, 4851 a.u, 3386 a.u, and 1403 a.u at 22.46°, 23.14°, 27.02°, 29.46°, 31.42°, 31.46°, and 56.54°, respectively. Apparently, these drug representing sharp peaks were disappeared in the corresponding XRD patterns of drug-loaded formulations probably because drug fraction was lesser as compared to biomineralized calcium carbonate or the drug was entrapped inside biomineralized calcium carbonate hollow composite fabric or both factors had their contributed influence. XRD results were consistent with the FTIR spectrum which also showed disappearance of absorption peaks of the drug after biomineralization process.

Scanning electron microscopy

Morphological analysis of the three paracetamol-loaded formulations F1, F2 and F3 having varying concentrations of quince hydrogel was accomplished by scanning electron microscopy. Calcium carbonate crystals with exposed crystalline faces (104) were observed that depicted calcite formation in quince hydrogel after biomineralization. The physical appearance of calcium carbonate crystals was homogenous in all the formulations as shown in Fig. 5. The magnified images of the formulations demonstrated that increase in quince hydrogel concentration shifts the typical rhombohedral shape of calcium carbonate crystals to somewhat spherical aggregates. Formulations F1 and F2 showed larger crystal size might be due to fast calcite growth rate at the lower quince hydrogel concentration [57]. The gel phase around the forming crystals limits the diffusion of particles in the solution thereby limiting the process of crystal formation. The surrounding gel environment thus plays a vital role in balancing the process of crystallization by creating a kinetic competition between the dissolution–precipitation of ions and the disintegration–crystallization of particles [58]. This restrictive property is much stronger in formulations having higher gel concentration as compared to those with lower gel concentration which is the reason why spherical calcite aggregates are seen in higher gel concentration, while single irregular crystals are visible in formulation having lower concentration [57].

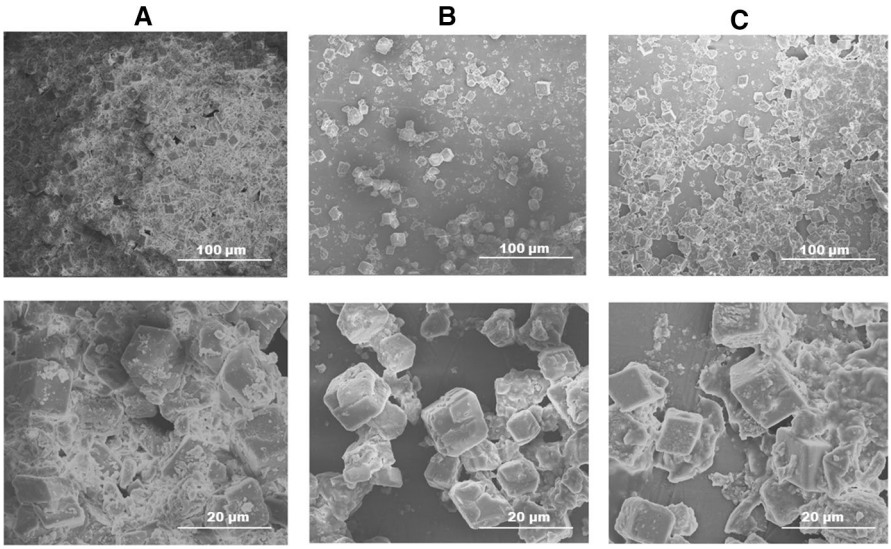

Fig. 5 SEM images of the drug-loaded $CaCO_3$-Q composites **A** F1 = drug-loaded CaCO3-Q composite containing 0.005% quince **B** F2 = drug-loaded $CaCO_3$-Q composite containing 0.05% quince **C** F3 = drug-loaded $CaCO_3$-Q composite containing 0.5% quince. Upper row images captured at 1000 × magnification; lower row images captured at 5000 × magnification

In vitro drug release study

There are numerous factors that influence bioavailability of the drug and among them physicochemical properties of the active pharmaceutical ingredient (API) itself and type of dosage form are the most important in product development process. Oral liquid dosage forms usually have more rate and extend of drug to reach in systemic circulation than the oral solid dosage forms. Obviously, the drug is needed to be dissolved before absorbed, however, solubility and dissolution rate are influenced by pH. After oral administration, the drug is passed through various pH conditions, i.e. acidic pH in stomach (pH 1.2) and 6.8 pH in small intestine. Previous study of swelling/deswelling behaviour of quince seed mucilage, where nominal swelling was observed in acidic medium (pH 1.2) and high swelling was observed in PBS buffer pH6.8 [32], demonstrated quince seed mucilage as a retarding material to control drug release in acidic medium. On the other hand, mesoporous calcium carbonate is promising oral drug carrier for its nature of porous structure, large surface area, capacity to protect encapsulated materials, biocompatibility and biodegradability properties. However, calcium carbonate particles are soluble in acidic medium. Non-steroidal anti-inflammatory drugs (NSAIDs) are prescribed in various disorders. However, long-term use of NASAIDs in chronic diseases may increase risk of gastrointestinal track ulcer. Hence, developing a safe oral therapy of NASAID is the demand to overcome NSAIDs-associated ulcer burden.

In this study, biomineralized calcium carbonate-quince ($CaCO_3$-Q) composites were designed for sustained and colon targeted delivery of paracetamol. Drug

release study was carried out in acidic medium pH 1.2 (0.1 N HCl) and PBS buffer pH 6.8.

After 4 h, the average drug release of 22.05%, 12.82% and 7.89% was witnessed in acidic medium from formulations F1, F2, and F3, respectively. Whereas, 36.85%, 30.32% and 14.30% of average drug release in PBS was observed from formulations F1, F2, and F3, respectively, as shown in Fig. 6A. A 50% of the drug release in PBS at pH 6.8 was observed after 5 h, 6.75 h and 9 h from the formulations F1, F2, and F3, respectively. At the end of the study period (12 h), the average drug release in the acidic medium was restricted to less than 40%, 30% and 20% from the formulations F1, F2 and F3, respectively. During the study period (12 h), overall scenario was that these three formulations F1, F2, and F3 displayed considerably low release rate in 0.1 N HCl (pH 1.2), i.e. 37.90 ± 6.18, 25.64 ± 2.46, and 15.17 ± 1.79, respectively; whereas the average drug release in PBS at pH 6.8 was reached up to 95.31 ± 3.05, 81.86 ± 2.68, and 64.17 ± 14.72, respectively, as shown in Fig. 6B. The order of release rate appears to be F1 > F2 > F3 which depicts that the formulation with the highest concentration of quince seed mucilage powder in the formulation, i.e. 0.5% in formulation F3 controlled more drug release in both the media. This quince seed mucilage concentration-dependent control of drug release in PBS at pH 6.8 and retardation of drug release in acidic medium notably were due to swelling/deswelling behaviour of quince seed mucilage under the influence of protonation and deprotonation of carboxyl group ($–COO^-$) of glucuronic acid residues present in quince seed mucilage. The literature-based studies have demonstrated that the ionized forms of carbonyl group ($–COO^-$) generate electrostatic repulsive forces in the polymeric chain of quince hydrogel networks, hence, thereby opening the pores and flushing the media in the gel networks to facilitate swelling of the gel, which leads to dissolution and release of the drug in the basic medium. On the other hand, the carboxyl group (–COOH) is protonated in the acidic medium, causing a decrease in repulsive forces and locking the gel networks to flush the media in; leading to retard drug release in acidic medium [32]. Moreover, the highest drug loading (30% by weight) with entrapment efficiency of more than 80% was achieved in all the formulations as stated above in drug loading and entrapment efficiency section. This high

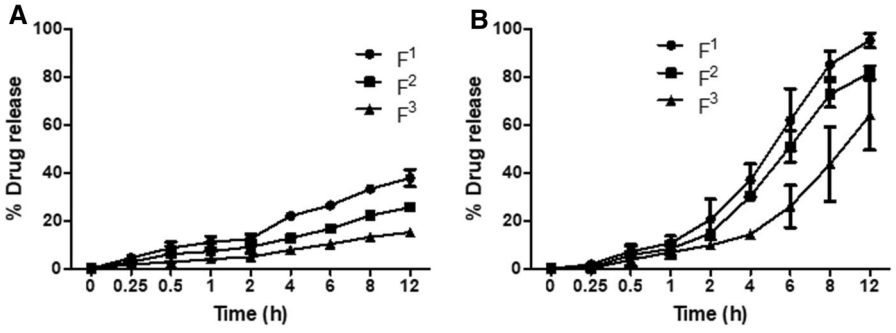

Fig. 6 Drug release from the developed $CaCO_3$-Q composite **A** acidic medium (O.1 N HCl); **B** PBS at pH 6.8. F1 = drug-loaded $CaCO_3$-Q composite containing 0.005% quince; F2 = drug-loaded $CaCO_3$-Q composite containing 0.05% quince; F3 = drug-loaded $CaCO_3$-Q composite containing 0.5% quince

drug payload and entrapment efficiency were obviously due to increase in porosity networks in quince hydrogel under the influence of biomineralized calcium carbonate. It has been demonstrated that mesoporous inorganic materials such as calcium carbonate play promising role in oral drug delivery by providing salient features to their corresponding formulation including increase surface area and porosity that result in a high drug loading capacity. Moreover, adsorption of drug inside the nanoporous structure of the inorganic carrier causes the drug to remain in an amorphous state, thereby increasing the dissolution rate [37].

Drug release kinetics

To understand the drug release behaviour from the developed $CaCO_3$-Q composite hollow networks, various in vitro kinetic models were applied such as zero order, 1st order, Higuchi, Korsmeyer-Peppas, Weibull, Logistic, Gompertz, and Probit.

Generally, R^2 value via regression analysis is used to find the best-fit model. Herein, we elected various parameters from 'goodness of fit' table of regression analysis such as R^2, adjusted R^2, SS (sum of squares), and constants (α and β), whereas 'n' value from Krosmeyer-Peppas model was considered for mechanism of drug release. Akaike information criteria (AIC) were also computed to find the best-fit model. In case of acidic medium (0.1 N HCl), the Weibull model was considered the best fit for formulation F1 and F3 which showed the highest adjusted R^2 values of 0.9993 and 0.9833 and the lowest AIC values of 2.688 and 14.0579, respectively. The F2 formulation was found the best fit for Probit model based on the highest adjusted R^2 value of 0.9933 and the lowest AIC value of 22.6983. In addition, no significant change in β values was observed for all the formulations in Weibull model ($\beta < 1$) (Table 2). Hence, all the formulations (F1, F2, and F3) were found the best fit by Weibull model. The Korsmeyer-Peppas model explained non-Fickian diffusion ($0.43 < n < 0.85$) of drug release mechanism from all the developed systems, i.e. F1 ($n = 0.534$), F2 ($n = 0.591$), and F3 ($n = 0.591$). All in vitro kinetic parameters are listed in Table 2.

Similarly, in case of PBS pH 6.8, the F1 formulation was found to be the best fit by Korsmeyer-Peppas model based on the highest adjusted R^2 value of 0.9890 and the lowest AIC value of 26.1695, respectively. The F2 formulation was best fitted by Probit model that showed the highest adjusted $R^2 = 0.9996$ in association with the lowest AIC = 13.4481. In contrast, F3 formulation best fitted by Gopmertz model showed the highest adjusted $R^2 = 96.4498$ and the lowest AIC = 28.6081. The diversity in kinetic behaviour of all the three formulations might be due to change in porosity of the resultant composite after biomineralization of calcium carbonate at different concentration of quince hydrogel, i.e. 0.005%, 0.05%, and 0.5% in F1, F2, and F3 formulations, respectively. All the three formulations showed higher than 1 value of coefficient β in Weibull model that was an indication of complex drug release mechanism [59] (Table 3). This complex behaviour of drug release was also correlated with the coefficient 'n' of Korsmeyer-Peppas model where $n > 1$ suggested Supper Case II transport mechanism of drug release [60]. Therefore, the value of 'n' of F1, F2, and F3 formulations, i.e. 1.031, 1.092, and 1.265, respectively, suggested

Table 2 In vitro kinetic model parameters for drug release in acidic medium (0.1 N HCl)

Formulation	Zero order	1st order	Higuchi	Korsmeyer-Peppas	Weibull	Logistic	Gompertz	Probit	Parameters
F1	0.7962	0.8681	0.9698	0.9745	0.9994	0.9977	0.986	0.9942	R^2
F2	0.6954	0.7413	0.8942	0.9670	0.9675	0.9675	0.9606	0.9652	
F3	0.8541	0.8772	0.9773	0.8541	0.9854	0.9851	0.9767	0.9819	
F1	0.7962	0.8681	0.9698	0.9709	0.9993	0.9974	0.984	0.9933	Adjusted R^2
F2	0.6954	0.7413	0.8942	0.9623	0.9628	0.9629	0.955	0.9933	
F3	0.8541	0.8772	0.9773	0.8541	0.9833	0.983	0.9734	0.9793	
F1	297.3303	193.802	42.5606	36.5565	0.9014	3.2125	19.3467	8.0746	SS
F2	164.348	138.392	65.3057	19.0782	18.6696	18.5967	23.238	8.0746	
F3	32.8501	27.4723	5.6346	32.8501	3.5988	3.6426	5.5361	4.3551	
F1	52.6092	48.5426	35.7023	36.1121	2.6887	14.157	30.5793	22.6983	AIC
F2	41.5715	38.3541	38.4024	29.0013	28.6818	28.6229	31.7993	22.6983	
F3	33.1769	31.5905	15.9528	33.1769	14.0579	14.3121	18.5777	16.2922	
F1	n/a	n/a	n/a	n/a	9.607	− 2.198	2.295	− 1.279	a
F2	n/a	n/a	n/a	n/a	18.618	− 2.807	3.031	− 1.598	
F3	n/a	n/a	n/a	n/a	26.945	− 3.28	3.342	− 1.803	
F1	n/a	n/a	n/a	n/a	0.607	1.572	0.751	0.881	β
F2	n/a	n/a	n/a	n/a	0.646	1.618	0.7	0.867	
F3	n/a	n/a	n/a	n/a	0.604	1.455	0.519	0.713	

Table 3 In vitro kinetic model parameters for drug release in PBS pH 6.8

Formulation	Zero order	1st order	Higuchi	Korsmeyer-Peppas	Weibull	Logistic	Gompertz	Probit	Parameters
F1	0.9497	0.9514	0.8867	0.9909	0.9826	0.9736	0.9535	0.9716	R^2
F2	0.9628	0.9626	0.8762	0.9845	0.9794	0.9675	0.9947	0.9996	
F3	0.9549	0.9158	0.7964	0.9612	0.9557	0.9526	85.8253	0.942	
F1	0.9497	0.9514	0.8867	0.9890	0.9792	0.9698	0.9469	0.9676	Adjusted R^2
F2	0.9628	0.9626	0.8762	0.9815	0.9753	0.9851	0.9939	0.9996	
F3	0.9549	0.9158	0.7964	0.9547	0.9484	0.9458	96.4498	0.9337	
F1	566.073	521.531	1215.39	32.3369	61.464	292.391	513.705	313.925	SS
F2	308.7489	309.523	1007.21	36.6307	48.7877	100.566	40.6572	2.859	
F3	150.7206	342.075	882.036	40.5995	52.056	121.55	178.972	151.202	
F1	57.2698	57.8487	65.701	26.1695	30.7036	54.4864	59.7299	55.2	AIC
F2	52.6971	52.9932	64.0784	17.3519	17.492	45.3274	37.3363	13.4481	
F3	47.0006	53.5906	61.6225	33.5518	35.5934	45.9266	28.6081	48.0635	
F1	n/a	n/a	n/a	n/a	11.678	− 3.508	11.184	− 2.089	α
F2	n/a	n/a	n/a	n/a	15.38	− 2.824	4.092	− 1.685	
F3	n/a	n/a	n/a	n/a	63.584	− 4.498	15.908	− 2.693	
F1	n/a	n/a	n/a	n/a	1.266	5.349	3.918	3.203	β
F2	n/a	n/a	n/a	n/a	1.29	3.85	2.501	2.304	
F3	n/a	n/a	n/a	n/a	1.519	4.668	3.019	2.791	

Super Case II transport of drug from the developed composite systems in PBS pH 6.8. All in vitro kinetic parameters are listed in Table 3.

Conclusion

Hydrogels are regarded as 3-D networks of natural or synthetic polymers (organic material) with high water absorption properties. Most of the synthetic polymer-based hydrogels switch-on in acidic environment to release the drug. In contrast, calcium carbonate is a mineral (inorganic material) that has large surface area and large porosity. Like most of the synthetic polymer based hydrogels, calcium carbonate dissolves in stomach at acidic pH and releases the drug. Hence, these both systems have been found to be effective for pH responsive oral drug delivery of water-soluble drugs in the stomach. However, from the last few decades, organic–inorganic hybrid materials have attracted widespread attention from researchers to develop intelligent drug delivery system with feature of interests. Considering this, bioinspired materials are developed by biomineralization of calcium carbonate in the hydrogels. In this study, we reported composite system prepared by biomineralization of calcium carbonate in mucilage obtained from seed of naturally occurring quince plant. The developed composite showed restricted release of paracetamol in the acidic media, while a controlled fashion of drug release was observed in the basic media during the study period of 12 h. Study outcomes suggested the developed composite can be considered a novel drug carrier system for oral colon targeted delivery of hydrophilic/hydrophobic drugs. The restricted release of drug in an acidic medium and the controlled release fashion of drug in a basic medium make this composite an attractive model to overwhelm risk factor of NASAIDs-associated gastric ulcer. The in vitro kinetics suggested Super Case II drug transport mechanism of drug release. We also recommend a possible application of the developed composite for oral delivery of proteins and genes.

Supplementary Information The online version contains supplementary material available at https://doi.org/10.1007/s00289-022-04400-1.

Acknowledgements Not applicable.

Author contributions M.S. and A.A. contributed to conceptualization; R.K., M.U.F., S.A.K., and S.A. contributed to data curation; R.K., M.S., and A.A. contributed to writing original draft; M.S. and A.A. contributed to visualization and supervision; all authors contributed to writing—review and editing.

Funding There is no financial support for this work.

Availability of data and material Not applicable.

Code availability Not applicable.

Declarations

Conflicts of interest All the authors declare no conflict of interests.

Consent to participate Not applicable.

Consent for publication All authors give consent for the publication of manuscript in Polymer Bulletin.

Ethics approval Not applicable.

References

1. Fields E, Chard J, Murphy MS et al (2013) Assessment and initial management of feverish illness in children younger than 5 years: summary of updated NICE guidance. BMJ 22(346):f2866. https://doi.org/10.1136/bmj.f2866 (**PubMed PMID: 23697671**)
2. https://www.marketresearch.com/DataM-Intelligence-4Market-Research-LLP-v4207/Global-Paracetamol-30005076/ GPM
3. Pandolfi S, Simonetti V, Ricevuti G et al (2021) Paracetamol in the home treatment of early COVID-19 symptoms: a possible foe rather than a friend for elderly patients? J Med Virol 93(10):5704–5706. https://doi.org/10.1002/jmv.27158
4. Sestili P, Fimognari C (2020) Paracetamol-induced glutathione consumption: is there a link with severe covid-19 illness ? Front Pharmacol 11:1597. https://doi.org/10.3389/fphar.2020.579944
5. de Martino M, Chiarugi A (2015) Recent advances in pediatric use of oral paracetamol in fever and pain management. Pain Ther 4(2):149–168. https://doi.org/10.1007/s40122-015-0040-z (**PubMed PMID: 26518691**)
6. Mund ME, Quarcoo D, Gyo C et al (2015) Paracetamol as a toxic substance for children: aspects of legislation in selected countries. J Occup Med Toxicol 10(1):43. https://doi.org/10.1186/s12995-015-0084-3
7. Khazaeni SAB (2021) Acetaminophen toxicity. In: statpearls Treasure Island (FL): StatPearls Publishing; [Updated on 2021 Jul 18]. Available from: https://www.ncbinlmnihgov/books/NBK441917
8. Prescott LF (1980) Kinetics and metabolism of paracetamol and phenacetin. Br J Clin Pharmacol 10(Suppl 2):291S-298S. https://doi.org/10.1111/j.1365-2125.1980.tb01812.x (**PubMed PMID: 7002186**)
9. Shaw LR, Irwin WJ, Grattan TJ et al (2005) The effect of selected water-soluble excipients on the dissolution of paracetamol and ibuprofen. Drug Dev Ind Pharm 31(6):515–525. https://doi.org/10.1080/03639040500215784
10. Forrest JA, Clements JA, Prescott LF (1982) Clinical pharmacokinetics of paracetamol. Clin Pharmacokinet 7(2):93–107. https://doi.org/10.2165/00003088-198207020-00001 (**PubMed PMID: 7039926**)
11. Heading RC, Nimmo J, Prescott LF et al (1973) The dependence of paracetamol absorption on the rate of gastric emptying. Br J Pharmacol 47(2):415–421. https://doi.org/10.1111/j.1476-5381.1973.tb08339.x (**PubMed PMID: 4722050**)
12. Chen Y, Feng Y, Deveaux JG et al (2019) Biomineralization forming process and bio-inspired nanomaterials for biomedical application: a review. Minerals 9(2):68. https://doi.org/10.3390/min9020068
13. Asenath-Smith E, Li H, Keene EC et al (2012) Crystal growth of calcium carbonate in hydrogels as a model of biomineralization. Adv Funct Mater 22(14):2891–2914. https://doi.org/10.1002/adfm.201200300
14. Wang J, Song J, Ji Z et al (2020) The preparation of calcium carbonate with different morphologies under the effect of alkanolamide 6502. Coll Surf A: Physicochem Eng Asp 588:124392. https://doi.org/10.1016/j.colsurfa.2019.124392
15. Kırboga S, Öner M (2012) The inhibitory effects of carboxymethyl inulin on the seeded growth of calcium carbonate. Coll Surf B: Biointerfaces 91:18–25. https://doi.org/10.1016/j.colsurfb.2011.10.031
16. Xing X, Zhao Z, Shi X et al (2019) Studies of morphology and size of calcium carbonate crystals nucleating on surfaces of various materials. Crystallogr Rep 64(7):1150–1158. https://doi.org/10.1134/S1063774519070277
17. Bastrzyk A, Fiedot-Toboła M, Polowczyk I et al (2019) Effect of a lipopeptide biosurfactant on the precipitation of calcium carbonate. Colloids Surf B Biointerfaces 174:145–152. https://doi.org/10.1016/j.colsurfb.2018.11.009 (**PubMed PMID: 30448711**)

18. Kanoje B, Parikh J, Kuperkar K (2018) Crystallization study and morphology behaviour of calcium carbonate crystals in aqueous Surfactant-Pluronics® prototype. J Mater Res Technol 7(4):508–514. https://doi.org/10.1016/j.jmrt.2017.10.005
19. Jo Mk, Oh Y, Kim HJ et al (2020) Diffusion-controlled crystallization of calcium carbonate in a hydrogel. Cryst Growth Des 20(2):560–567. https://doi.org/10.1021/acs.cgd.9b00614
20. Gautam M, Santhiya D (2019) In-situ mineralization of calcium carbonate in pectin based edible hydrogel for the delivery of protein at colon. J Drug Deliv Sci Technol 53:101137. https://doi.org/10.1016/j.jddst.2019.101137
21. Qu F, Meng T, Dong Y et al (2019) Aqueous two-phase droplet-templated colloidosomes composed of self-formed particles via spatial confined biomineralization. ACS Appl Mater Interfaces 11(39):35613–35621. https://doi.org/10.1021/acsami.9b15086 (**PubMed PMID: 31505927**)
22. Boi S, Dellacasa E, Rouatbi N et al (2019) Multicompartment hydrogels for the local delivery of chemotherapic drugs. Stud Health Technol Inform 261:261–265 (**PubMed PMID: 31156127**)
23. Choi H, Hwang BW, Park KM et al (2020) Degradable nanomotors using platinum deposited complex of calcium carbonate and hyaluronate nanogels for targeted drug delivery. Part Part Syst Charact 37(1):1900418. https://doi.org/10.1002/ppsc.201900418
24. Elbaz NM, Owen A, Rannard S et al (2020) Controlled synthesis of calcium carbonate nanoparticles and stimuli-responsive multi-layered nanocapsules for oral drug delivery. Int J Pharm 574:118866. https://doi.org/10.1016/j.ijpharm.2019.118866
25. Samateh M, Pottackal N, Manafirasi S et al (2018) Unravelling the secret of seed-based gels in water: the nanoscale 3D network formation. Sci Rep 8(1):7315. https://doi.org/10.1038/s41598-018-25691-3
26. Choudhary PD, Pawar HA (2014) Recently investigated natural gums and Mucilages as pharmaceutical excipients: an overview. J Pharm 2014:204849–204849. https://doi.org/10.1155/2014/204849 (**PubMed PMID: 26556189**)
27. Prajapati VD, Jani GK, Moradiya NG et al (2013) Pharmaceutical applications of various natural gums, mucilages and their modified forms. Carbohydr Polym 92(2):1685–1699. https://doi.org/10.1016/j.carbpol.2012.11.021
28. Ashraf MU, Hussain MA, Muhammad G et al (2017) A superporous and superabsorbent glucuronoxylan hydrogel from quince (Cydonia oblanga): stimuli responsive swelling, on-off switching and drug release. Int J Biol Macromol 95:138–144
29. Vignon MR, Gey C (1998) Isolation, 1H and 13C NMR studies of (4-O-methyl-D-glucurono)-D-xylans from luffa fruit fibres, jute bast fibres and mucilage of quince tree seeds. Carbohyd Res 307(1–2):107–111
30. Ashraf MU, Muhammad G, Hussain MA, Bukhari SN, Cydonia OM (2016) A medicinal plant rich in phytonutrients for pharmaceuticals. Front Pharmacol 7:163. https://doi.org/10.3389/fphar.2016.00163 (**PubMed PMID: 27445806**)
31. Hakala TJ, Saikko V, Arola S et al (2014) Structural characterization and tribological evaluation of quince seed mucilage. Tribol Int 77:24–31. https://doi.org/10.1016/j.triboint.2014.04.018
32. Ashraf MU, Hussain MA, Bashir S et al (2018) Quince seed hydrogel (glucuronoxylan): Evaluation of stimuli responsive sustained release oral drug delivery system and biomedical properties. J Drug Deliv Sci Technol 45:455–465
33. Hosseinzadeh H, Mohammadi S (2015) Quince seed mucilage magnetic nanocomposites as novel bioadsorbents for efficient removal of cationic dyes from aqueous solutions. Carbohydr Polym 134:213–221. https://doi.org/10.1016/j.carbpol.2015.08.008
34. Tabrizi Hafez Moghaddas SM, Elahi B, Javanbakht V (2020) Biosynthesis of pure zinc oxide nanoparticles using Quince seed mucilage for photocatalytic dye degradation. J Alloys Compd 821:153519. https://doi.org/10.1016/j.jallcom.2019.153519
35. Kirtil E, Oztop MH (2016) Characterization of emulsion stabilization properties of quince seed extract as a new source of hydrocolloid. Food Res Int 85:84–94. https://doi.org/10.1016/j.foodres.2016.04.019
36. Ghadermazi R, Khosrowshahi Asl A, Tamjidi F (2019) Optimization of whey protein isolate-quince seed mucilage complex coacervation. Int J Biol Macromol 131:368–377. https://doi.org/10.1016/j.ijbiomac.2019.03.026
37. Trofimov AD, Ivanova AA, Zyuzin MV et al (2018) Porous inorganic carriers based on silica, calcium carbonate and calcium phosphate for controlled/modulated drug delivery: fresh outlook and future perspectives. Pharmaceutics 10(4):167. https://doi.org/10.3390/pharmaceutics10040167 (**PubMed PMID: 30257514**)
38. Rwei S-P, Anh THN, Chiang W-Y et al (2016) Synthesis and drug delivery application of thermo-and pH-sensitive hydrogels: poly (β-CD-co-N-isopropylacrylamide-co-IAM). Materials 9(12):1003

39. Pylypchuk IV, Daniel G, Kessler VG et al (2020) Removal of diclofenac, paracetamol, and carbamazepine from model aqueous solutions by magnetic sol–gel encapsulated horseradish peroxidase and lignin peroxidase composites. Nanomaterials 10(2):282. https://doi.org/10.3390/nano10020282 (**PubMed PMID: 32046049**)
40. Ghadami Jadval Ghadam A, Idrees M (2013) Characterization of CaCO3 nanoparticles synthesized by reverse microemulsion technique in different concentrations of surfactants. Iran J Chem Chem Eng (IJCCE) 32(3):27–35
41. Moghbel A, Tayebi M (2015) Quince seeds biopolymer: extraction, drying methods and evaluation. Jundishapur J Nat Pharm Prod 10(3):e25392
42. Hussain MA, Muhammad G, Haseeb MT et al (2019) Quince seed mucilage: a stimuli-responsive/smart biopolymer. Funct Biopolym, pp 1–22
43. Mahdavinia G, Bagheri Marandi G (2009) Synthesis of porous poly(acrylamide) hydrogels using calcium carbonate and its application for slow release of potassium nitrate. Express Polym Lett 3:279–285. https://doi.org/10.3144/expresspolymlett.2009.35
44. Burgina EB, Baltakhinov VP, Boldyreva EV et al (2004) IR spectra of paracetamol and phenacetin. 1. Theoretical and experimental studies. J Struct Chem 45(1):64–73. https://doi.org/10.1023/B:JORY.0000041502.85584.d5
45. Almurisi SH, Doolaanea AA, Akkawi ME et al (2020) Taste masking of paracetamol encapsulated in chitosan-coated alginate beads. J Drug Deliv Sci Technol 56:101520. https://doi.org/10.1016/j.jddst.2020.101520
46. Ali AMA, Khames A, Alrobaian MM et al (2018) Glucosamine-paracetamol spray-dried solid dispersions with maximized intrinsic dissolution rate, bioavailability and decreased levels of in vivo toxic metabolites. Drug Des Devel Ther 12:3071–3084. https://doi.org/10.2147/DDDT.S176099 (**PubMed PMID: 30275684**)
47. Shah R, Saha N, Kitano T et al (2014) Preparation of CaCO3-based biomineralized polyvinylpyrrolidone–carboxymethylcellulose hydrogels and their viscoelastic behavior. J Appl Polym Sci. https://doi.org/10.1002/app.40237
48. BrečevićLjerka FAA (1991) Infrared spectra of amorphous and crystalline calcium carbonate. Acta Chem Scand 45:1018–1024. https://doi.org/10.3891/acta.chem.scand.45-1018
49. Lai LS, Chao SJ (2000) A DSC study on the gel−sol transition of a starch and hsian-tsao leaf gum mixed system. J Agric Food Chem 48(8):3267–3274. https://doi.org/10.1021/jf991115t
50. Karunadasa KSP, Manoratne CH, Pitawala HMTGA et al (2019) Thermal decomposition of calcium carbonate (calcite polymorph) as examined by in-situ high-temperature X-ray powder diffraction. J Phys Chem Solids 134:21–28. https://doi.org/10.1016/j.jpcs.2019.05.023
51. Zimmermann B, Baranovic G (2011) Thermal analysis of paracetamol polymorphs by FT-IR spectroscopies. J Pharm Biomed Anal 54(2):295–302. https://doi.org/10.1016/j.jpba.2010.08.023 (**PubMed PMID: 20863645**)
52. Grasby SE (2003) Naturally precipitating vaterite (μ-CaCO3) spheres: unusual carbonates formed in an extreme environment. Geochim Cosmochim Acta 67(9):1659–1666. https://doi.org/10.1016/S0016-7037(02)01304-2
53. Chakrabarty D, Mahapatra S (1999) Aragonite crystals with unconventional morphologies. J Mater Chem 9(11):2953–2957. https://doi.org/10.1039/A905407C
54. Xie A-J, Yin H-S, Liu H-M et al (2018) Chinese quince seed gum and poly (N, N-diethylacryl amide-co-methacrylic acid) based pH-sensitive hydrogel for use in drug delivery. Carbohydr Polym 185:96–104. https://doi.org/10.1016/j.carbpol.2018.01.007
55. Ni M, Ratner BD (2008) Differentiation of calcium carbonate polymorphs by surface analysis techniques - An XPS and TOF-SIMS study. Surf Interface Anal 40(10):1356–1361. https://doi.org/10.1002/sia.2904 (**PubMed PMID: 25031482**)
56. . (File No 5–586)-Join Committee on Powder Diffraction Standard (JCPDS) (1996) International centre for diffraction data
57. Ma Y, Feng Q, Bourrat X (2013) A novel growth process of calcium carbonate crystals in silk fibroin hydrogel system. Mater Sci Eng, C 33(4):2413–2420
58. Gal A, Habraken W, Gur D et al (2013) Calcite crystal growth by a solid-state transformation of stabilized amorphous calcium carbonate nanospheres in a hydrogel. Angew Chem Int Ed 52(18):4867–4870
59. Weibull W (1951) A statistical distribution function of wide applicability. J Appl Mech 18:293–297
60. Korsmeyer RW, Gurny R, Doelker E et al (1983) Mechanisms of solute release from porous hydrophilic polymers. Int J Pharm 15(1):25–35. https://doi.org/10.1016/0378-5173(83)90064-9